JACS
JOURNAL OF THE AMERICAN CHEMICAL SOCIETY

Communication

pubs.acs.org/JACS

Epoxide Hydrolase–Lasalocid A Structure Provides Mechanistic Insight into Polyether Natural Product Biosynthesis

Fong T. Wong,[§,∥] Kinya Hotta,[†,∥,#] Xi Chen,[†] Minyi Fang,[†] Kenji Watanabe,[⊥] and Chu-Young Kim*[,†,‡]

[†]Department of Biological Sciences, National University of Singapore, 117543 Singapore
[‡]Synthetic Biology Research Consortium, National University of Singapore, 117456 Singapore
[§]Molecular Engineering Lab, Biomedical Sciences Institutes, 138673 Singapore
[⊥]Division of Pharmaceutical Sciences, University of Shizuoka, Shizuoka 422-8526, Japan

Supporting Information

ABSTRACT: Biosynthesis of some polyether natural products involves a kinetically disfavored epoxide-opening cyclic ether formation, a reaction termed anti-Baldwin cyclization. One such example is the biosynthesis of lasalocid A, an ionophore antibiotic polyether. During lasalocid A biosynthesis, an epoxide hydrolase, Lsd19, converts the bisepoxy polyketide intermediate into the tetrahydrofuranyl-tetrahydropyran product. We report the crystal structure of Lsd19 in complex with lasalocid A. The structure unambiguously shows that the C-terminal domain of Lsd19 catalyzes the intriguing anti-Baldwin cyclization. We propose a general mechanism for epoxide selection by ionophore polyether epoxide hydrolases.

Polyether natural products contain cyclic ether moieties that are formed via epoxide ring-opening reactions. According to Baldwin's rules, epoxide ring-opening closure that forms the smaller ring system, i.e., an *exo* cyclization, is generally favored over the *endo* cyclization.[1,2] This is verified by kinetic experiments in neutral water where the competing *exo* and *endo* mechanisms are first and second orders, respectively.[3] Intriguingly, some polyether natural products contain cyclic ether rings that are likely produced by the kinetically disfavored *endo* cyclization reaction. For example, brevetoxin B is thought to be formed by 10 disfavored, stereospecific anti-Baldwin epoxide-opening *endo* ring-closure reactions.[4] Polyethers exhibit a wide range of useful biological activities, such as antifungal, anticancer and neuroprotective activity. The ability to bioengineer polyether natural products or mimic their biosynthesis offers new opportunities for drug discovery. However, molecular mechanism of the disfavored epoxide-opening cyclization that takes place during polyether biosynthesis remains poorly understood.[5] To elucidate this mechanism and its specificities, we have investigated the biosynthesis of lasalocid A which contains one five-membered cyclic ether presumably formed by *exo* cyclization and one six-membered cyclic ether presumably formed by *endo* cyclization.[6]

Recently, the *Streptomyces lasaliensis* gene cluster for lasalocid A biosynthesis has been elucidated (Figure S1, Supporting Information).[7,8] This biosynthetic pathway is expected to produce a linear 12-carbon polyketide chain that subsequently undergoes aromatization to form the 3-methylsalicylate head-group, giving rise to prelasalocid A. Next, an epoxidase, Lsd18, converts the two E-olefins into epoxides to give bisepoxyprelasalocid A. Finally, an epoxide hydrolase, Lsd19, catalyzes two consecutive epoxide-opening cyclization reactions, one *exo* cyclization and one anti-Baldwin-type *endo* cyclization, on bisepoxyprelasalocid A to give the final product Lasalocid A (Scheme 1).[9] Exact timing and mechanisms of the cyclizations remain ill-defined.[10]

Scheme 1. Proposed Mechanism of Cyclic Ether Formation during Lasalocid A Biosynthesis

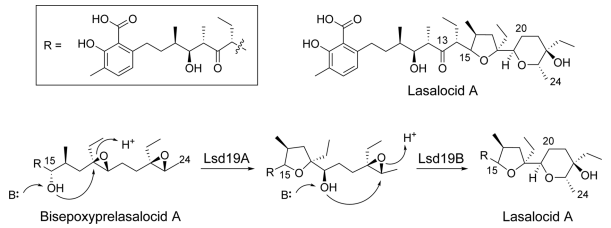

We have previously reported the crystal structure of Lsd19 in complex with a bisepoxide substrate analogue that has an oxazolidinone appendage in place of the 3-methylsalicylate group of the native substrate (PDB code: 3RGA).[11] In that structure, the unreacted bisepoxide substrate is seen in the 5-*exo* cyclization site (Lsd19A) while an unexpected tetrahydrofuran–tetrahydrofuran (THF–THF) product was found in the 6-*endo* cyclization site (Lsd19B). Therefore, it was not possible to directly elucidate the mechanism of tetrahydropyran (THP) formation. In this study, we present the first atomic structure of Lsd19 in complex with its native tetrahydrofuran–tetrahydropyran (THF–THP) product, lasalocid A.

Crystal structure of Lsd19–lasalocid A complex (PDB code: 4RZM) was determined to 2.33 Å resolution with final R_{work} and R_{free} values of 0.177 and 0.207, respectively (Table S1). Lsd19 is composed of two structurally homologous domains; an N-terminal Lsd19A domain and a C-terminal Lsd19B domain, arranged in a head-to-tail manner (Figure 1a). The substrate binding pocket of Lsd19A is unoccupied while Lsd19B contains the natural product lasalocid A (Figure 1b). This observation supports previous biochemical studies which

Received: November 5, 2014
Published: December 23, 2014

DOI: 10.1021/ja511374k
J. Am. Chem. Soc. 2015, 137, 86–89

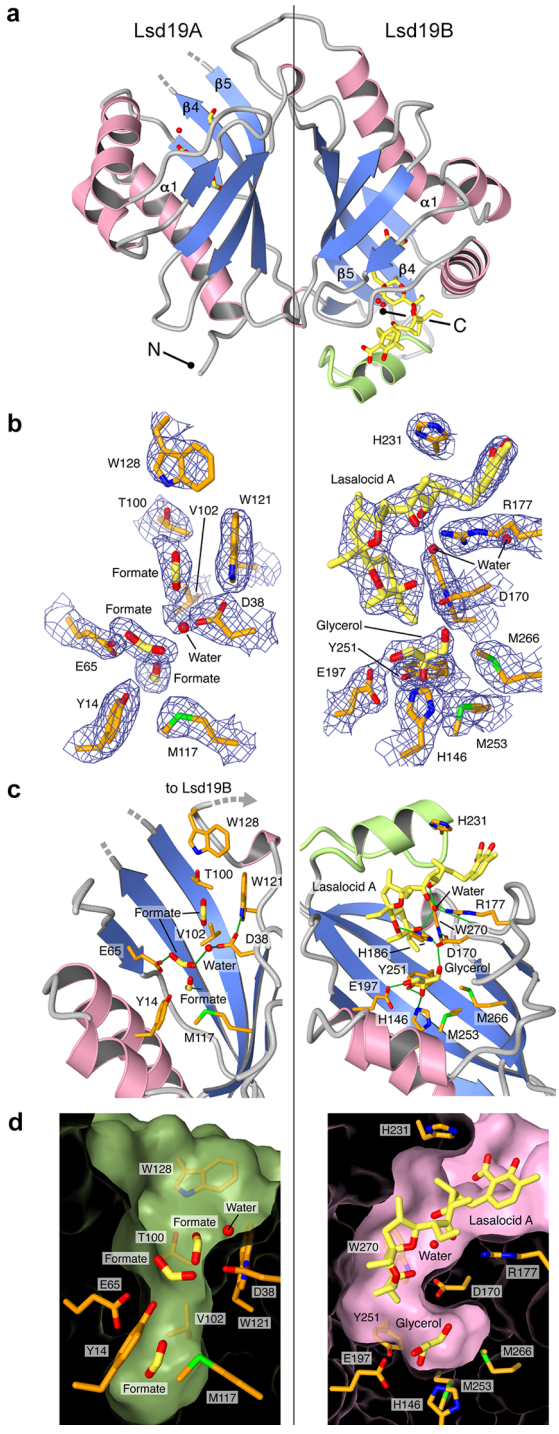

Figure 1. Lsd19–lasalocid A complex structure. (a) Overall fold of Lsd19. α-helices and β-sheets are shown in pink and blue, respectively. The loop-helix-loop present only in Lsd19B is highlighted in green. Carbon atoms of the ligand and protein are shown in yellow and orange, respectively. Oxygen and nitrogen atoms are represented by red and blue segments, respectively. (b) 2Fo–Fc electron density map, contoured at 1.6σ, of the active site pocket. (c,d) Ligand–protein interaction in the substrate binding pocket.

showed that Lsd19A catalyzes the initial 5-*exo* cyclization of the internal epoxide of bisepoxyprelasalocid A while Lsd19B catalyzes the subsequent anti-Baldwin 6-*endo* cyclization of the terminal epoxide to yield the final THF–THP product.[9] Lasalocid A is bound to the Lsd19B active site via multiple hydrogen bonds (Figure 1c). These include H-bond between the carbonyl oxygen O13 of lasalocid A with the side chain of Arg177, water-mediated H-bonds between the alcohol oxygen O11 of lasalocid A with the Asp170 backbone carbonyl oxygen and the terminal alcohol O22 of lasalocid A. O22 also forms a bifurcated H-bond with the side chain of Asp170 and His186. His186 side chain also forms an H-bond with the ether oxygen of the THP ring of Lasalocid A. Interestingly, the 3-methylsalicylate moiety does not make any specific interactions with Lsd19, suggesting that this moiety might not be necessary for substrate loading.

Although the Lsd19A active site in the current structure contains only buffer molecules while that in the Lsd19–analogue structure contains the bisepoxide substrate analogue, Lsd19A active site residues in the two structures adopt highly similar conformations (RMSD = 0.57 Å for 17 residues lining the binding pocket). Therefore, we hypothesize that Lsd19A employs a lock-and-key type substrate binding. Lsd19B active site in the current structure contains lasalocid A while that in the Lsd19–analogue complex structure contains the THF–THF product analogue. In the current structure, Arg177 is shifted to accommodate the larger 3-methylsalicilate headgroup of lasalocid A. Additionally, imidazole group of His186 is rotated by 90° which allows H-bond formation with both lasalocid A and the THF–THF product analogue despite significant differences in the structure and conformation of these two ligands. For Lsd19B, we cannot eliminate the possibility of an induced fit substrate binding since the vacant Lsd19B structure is not available. However, lack of large conformational changes, while interacting with two substantially different ligands, suggests that the Lsd19B pocket is capable of accommodating different ligands with minimal active site rearrangement. This is similar to the minimal conformational changes that the active site of the structurally related ketosteroid isomerase undergoes upon ligand binding.[12]

In the current structure, lasalocid A is shifted away from the putative catalytic residues (His146, Asp170, Glu197, Tyr251) and closer to the substrate binding pocket entrance of Lsd19B (Figure 1d) compared to the position of THF–THF analogue in the Lsd19–analogue structure. Interestingly, conformation of Lsd19-bound lasalocid A is nearly identical to that of free lasalocid A (Figure 2), suggesting that lasalocid A in the current structure is in its energy-minimum conformation. RMSD between the THF–THP portions (C12–24, Scheme 1) is 0.41 Å.

Every cyclic polyether ionophore biosynthetic gene cluster reported to date contains at least one putative polyether epoxide hydrolase (PEH), giving weight to the Cane–Westley–Celmer theory[14] of polyether biosynthesis. To

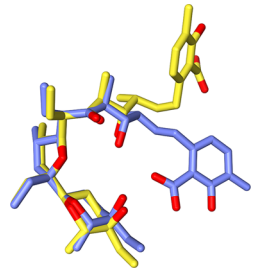

Figure 2. Conformation of Lsd19 bound lasalocid A (yellow) and conformation of free lasalocid A sodium salt[13] (purple).

DOI: 10.1021/ja511374k
J. Am. Chem. Soc. 2015, 137, 86–89

compare ionophore PEHs, we have constructed a phylogenetic tree (Figure 3). It clearly shows that the PEHs can be clustered

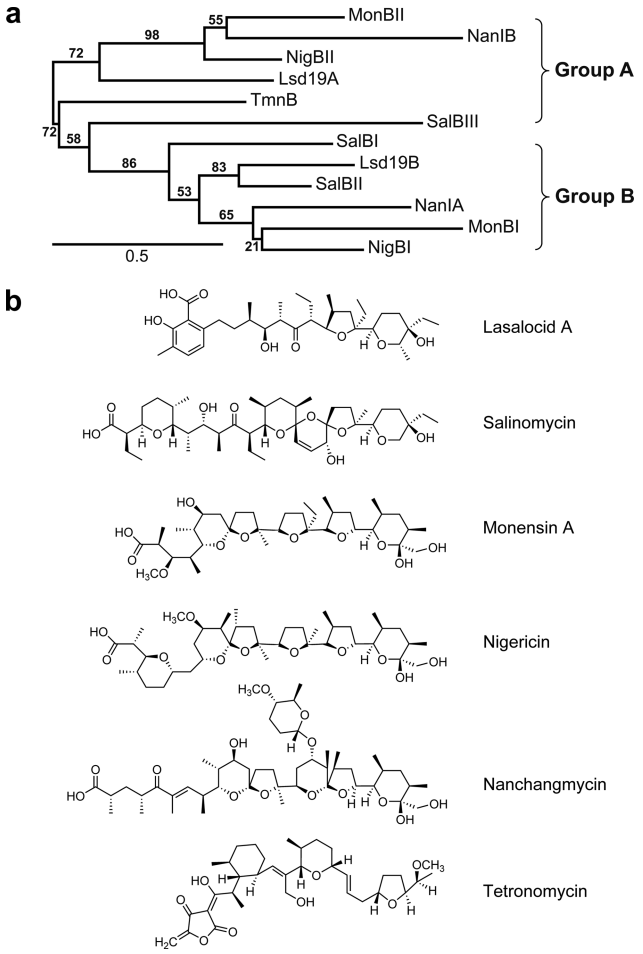

Figure 3. (a) Phylogenetic tree of polyether epoxide hydrolases. The bootstrap support values are shown in red. Biosynthetic gene cluster for lasalocid A (Lsd19)[7] and nachangmycin (NanI)[16] each contain one gene that encodes two PEH domains that are fused in tandem. Gene cluster for monensin (MonBI, MonBII),[17] nigericin (NigBI, NigBII),[18] salinomycin (SalBI, SalBII, SalBIII)[19,20] and tetronomycin (TmnB)[21] biosynthesis contain multiple single-domain PEH proteins. Sequence alignment of the epoxide hydrolases is provided in Figure S2. (b) Chemical structure of the respective ionophore polyether natural products.

into two distinct clades, group A and group B. Lsd19A (group A) and Lsd19B (group B) share a highly similar active site architecture but have different substrate binding pocket depths and therefore different pocket cavity volumes (Lsd19A = 416 Å^3, Lsd19B = 320 Å^3). This structural variation is predicted to allow Lsd19A to selectively transform the internal epoxide of bisepoxyprelasalocid A and Lsd19B to selectively transform the terminal epoxide of the same substrate molecule. Biosynthesis of all ionophore polyethers we have examined, with the exception of tetronomycin, involves at least one predicted group A PEH and one group B PEH.

We have built three-dimensional models of the various ionophore polyether producing PEH domains using the comparative protein structure modeling program MODELLER[15] based on our Lsd19−lasalocid A crystal structure (Figures 4, S3−S6). These homology models were used to calculate the substrate binding cavity volume of each PEH

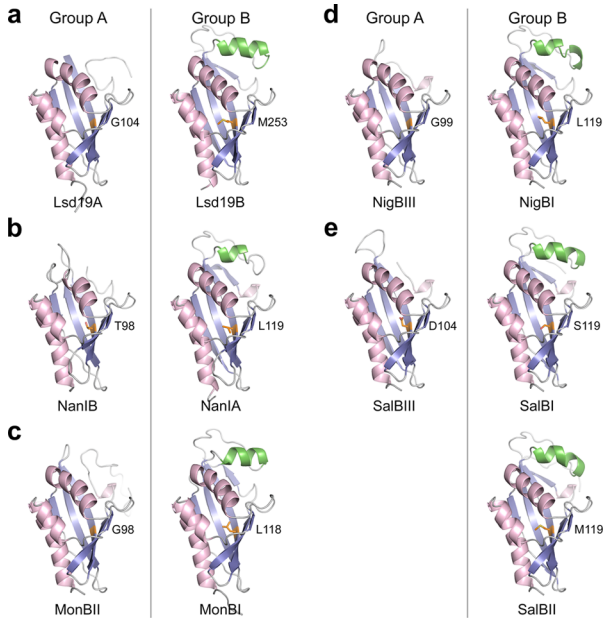

Figure 4. Structural comparison of PEHs involved in the biosynthesis of (a) lasalocid A, (b) nanchangmycin, (c) monensin, (d) nigericin, and (e) salinomycin. Lsd19AB (PDB code: 4RZM) and MonBI (PDB code: 3WMD[24]) are X-ray crystal structures. The remaining PEH structures are models generated using MODELLER[15] and verified with ERRAT.[25] Color scheme of the structures is same as in Figure 1. Differences in cavity depth can be contributed to Gly104 (Lsd19A) versus Met253 (Lsd19B). Similar trend is observed at the equivalent site of other PEHs.

enzyme. Predicted active site cavity volumes for Lsd19A-like enzymes (group A) ranges from 300 to 800 Å^3 while cavity volumes for Lsd19B-like enzymes (group B) ranges from 200 to 400 Å^3 (Table S2). Differences in cavity volume can be attributed to the presence of bulky Met or Leu at the bottom of the binding pocket in Lsd19B-like enzymes (group B) in place of Ala or Gly or Thr found at the bottom of Lsd19A-like enzymes (group A). This arrangement concurs with the epoxide position in the substrate. The deeper pocket allows for cyclization of the internal epoxide group while the shallow pocket ensures the active site residues act only on the terminal epoxide. This also correlates with the residue depth calculations for the highly conserved Asp−Glu−Tyr/His catalytic triad (Table S3). The conserved histidine (His146 in Lsd19) in the Lsd19B-like enzymes are placed, on average, 1.9 Å further away from bulk solvent, compared to their counterpart tyrosine (Tyr14 in Lsd19) in the Lsd19A-like enzymes. The extra distance from bulk solvent is predicted to allow Lsd19B-like enzymes to better accommodate the substrate and access the terminal epoxide. This concurs with the presence of a conserved extra loop-helix-loop, found only in Lsd19B-like PEHs, which is thought to provide additional binding surface for the bound substrate.[11]

The similar predicted catalytic mechanisms for *exo*- and *endo*-catalyzing active sites suggest that it would require more residues, specific substrate arrangement or specific substrate functionality to catalyze the anti-Baldwin reactions. One possible factor could be the precise arrangement of the substrate in the active site. Jamison and colleagues demonstrated that *endo* ring closure could proceed preferentially in the presence of hydrogen-bonding water molecules at near neutral pH for polyepoxide substrates when attached to a templating

DOI: 10.1021/ja511374k
J. Am. Chem. Soc. 2015, 137, 86−89

group that restricts the conformation of the substrates,[22] indicating that such energetically disfavored reactions can proceed stereospecifically under a biologically relevant condition. In addition, catalytic antibodies that catalyze a disfavored 6-*endo*-tet reaction have been successfully developed, demonstrating that enzymes are also capable of catalyzing this type of reaction.[23] Comparison of product analogue−Lsd19B and lasalocid A−Lsd19B complexes shows that the conformation of active site residues are minimally changed while conformational changes are apparent in the unique-loop-helix-loop's interactions with the terminal groups of the ligands (Figure 1b). Combined, these observations suggest that the precise three-dimensional arrangement of the substrate is highly relevant for preferential 6-*endo* cyclization. More detailed biochemical and structural characterizations of epoxide hydrolases will be necessary to gain a more complete understanding of exactly how these seemingly simple enzymes can differentiate and catalyze specific cyclization reactions, some of which are kinetically disfavored, on complex polyketide substrates.

■ ASSOCIATED CONTENT

Ⓢ Supporting Information

Experimental procedures and structure analysis data. This material is available free of charge via the Internet at http://pubs.acs.org.

■ AUTHOR INFORMATION

Corresponding Author

chuyoung@nus.edu.sg

Present Address

[#](For K.H.) School of Biosciences, University of Nottingham Malaysia Campus, Selangor 43500, Malaysia.

Author Contributions

[‖]F.T.W. and K.H. contributed equally.

Notes

The authors declare no competing financial interest.

■ ACKNOWLEDGMENTS

Data collection was performed at beamline 7-1 of the Stanford Synchrotron Radiation Lightsource. We thank Dr. I. I. Mathews (SSRL) for assistance with X-ray data collection and processing. This work was supported by the Singapore Ministry of Education Academic Research Fund (C.-Y.K.).

■ REFERENCES

(1) Baldwin, J. E. *J. Chem. Soc., Chem. Commun.* **1976**, 734−736.
(2) Baldwin, J. E.; Kruse, L. I. *J. Chem. Soc., Chem. Commun.* **1977**, *0*, 233−235.
(3) Morten, C. J.; Byers, J. A.; Van Dyke, A. R.; Vilotijevic, I.; Jamison, T. F. *Chem. Soc. Rev.* **2009**, *38*, 3175−3192.
(4) Nakanishi, K. *Toxicon* **1985**, *23*, 473−479.
(5) Ueberbacher, B. T.; Hall, M.; Faber, K. *Nat. Prod Rep.* **2012**, *29*, 337−350.
(6) Minami, A.; Oguri, H.; Wantanabe, K.; Oikawa, H. *Curr. Opin. Chem. Biol.* **2013**, *17*, 555−561.
(7) Migita, A.; Watanabe, M.; Hirose, Y.; Watanabe, K.; Tokiwano, T.; Kinashi, H.; Oikawa, H. *Biosci., Biotechnol., Biochem.* **2009**, *73*, 169−176.
(8) Smith, L.; Hong, H.; Spencer, J. B.; Leadlay, P. F. *ChemBioChem* **2008**, *9*, 2967−2975.
(9) Minami, A.; Migita, A.; Inada, D.; Hotta, K.; Watanabe, K.; Oguri, H.; Oikawa, H. *Org. Lett.* **2011**, *13*, 1638−1641.
(10) Tosin, M.; Smith, L.; Leadlay, P. F. *Angew. Chem., Int. Ed. Engl.* **2011**, *50*, 11930−11933.
(11) Hotta, K.; Chen, X.; Paton, R. S.; Minami, A.; Li, H.; Swaminathan, K.; Mathews, I. I.; Watanabe, K.; Oikawa, H.; Houk, K. N.; Kim, C.-Y. *Nature* **2012**, *483*, 355−358.
(12) Ha, N. C.; Choi, G.; Choi, K. Y.; Oh, B. H. *Curr. Opin. Struct. Biol.* **2001**, *11*, 674−678.
(13) Shui, X.; Eggleston, D. S. *Acta Crystallogr.* **1995**, *C51*, 805−809.
(14) Cane, D. E.; Celmer, W. D.; Westley, J. W. *J. Am. Chem. Soc.* **1983**, *105*, 3594−3600.
(15) Eswar, N.; Webb, B.; Marti-Renom, M. A.; Madhusudhan, M. S.; Eramia, D.; Shen, M. Y.; Pieper, U.; Sali, A. *Curr. Protoc. Protein Sci.* **2007**, 2.
(16) Sun, Y.; Zhou, X.; Dong, H.; Tu, G.; Wang, M.; Wang, B.; Deng, Z. *Chem. Biol.* **2003**, *10*, 431−441.
(17) Oliynyk, M.; Stark, C. B.; Bhatt, A.; Jones, M. A.; Hughes-Thomas, Z. A.; Wilkinson, C.; Oliynyk, Z.; Demydchuk, Y.; Staunton, J.; Leadlay, P. F. *Mol. Microbiol.* **2003**, *49*, 1179−1190.
(18) Harvey, B. M.; Mironenko, T.; Sun, Y.; Hong, H.; Deng, Z.; Leadlay, P. F.; Weissman, K. J.; Haydock, S. F. *Chem. Biol.* **2007**, *14*, 703−714.
(19) Yurkovich, M. E.; Tyrakis, P. A.; Hong, H.; Sun, Y.; Samborskyy, M.; Kamiya, K.; Leadlay, P. F. *ChemBioChem* **2012**, *13*, 66−71.
(20) Jiang, C.; Wang, H.; Kang, Q.; Liu, J.; Bai, L. *Appl. Environ. Microbiol.* **2012**, *78*, 994−1003.
(21) Demydchuk, Y.; Sun, Y.; Hong, H.; Staunton, J.; Spencer, J. B.; Leadlay, P. F. *ChemBioChem* **2008**, *9*, 1136−1145.
(22) Vilotijevic, I.; Jamison, T. F. *Science* **2007**, *317*, 1189−1192.
(23) Janda, K. D.; Shevlin, C. G.; Lerner, R. A. *Science* **1993**, *259*, 490−493.
(24) Minami, A.; Ose, T.; Sato, K.; Oikawa, A.; Kuroki, K.; Maenaka, K.; Oguri, H.; Oikawa, H. *ACS Chem. Biol.* **2014**, *9*, 562−569.
(25) Colovos, C.; Yeates, T. O. *Protein Sci.* **1993**, *2*, 1511−1519.

DOI: 10.1021/ja511374k
J. Am. Chem. Soc. 2015, 137, 86−89